Quaternary Structure of V1 and F1 ATPase: Significance of Structural Homologies and Diversities†

ARTICLE *in* BIOCHEMISTRY · DECEMBER 1998

Impact Factor: 3.02 · DOI: 10.1021/bi982367a · Source: PubMed

8 AUTHORS, INCLUDING:

Markus Huss
Universität Osnabrück
44 PUBLICATIONS **1,228** CITATIONS
SEE PROFILE

Michel Henri Jean Koch
European Molecular Biology Laboratory
413 PUBLICATIONS **16,098** CITATIONS
SEE PROFILE

Helmut Wieczorek
Universität Osnabrück
101 PUBLICATIONS **3,806** CITATIONS
SEE PROFILE

Vladimir Vladimirovich Volkov
Russian Academy of Sciences
152 PUBLICATIONS **3,539** CITATIONS
SEE PROFILE

Quaternary Structure of V_1 and F_1 ATPase: Significance of Structural Homologies and Diversities†

Dmitri I. Svergun,‡,§ Stephanie Konrad,|| Markus Huss,⊥ Michel H. J. Koch,‡ Helmut Wieczorek,⊥ Karlheinz Altendorf ,|| Vladimir V. Volkov,§ and Gerhard Grüber*,||

European Molecular Biology Laboratory, Hamburg Outstation, Notkestrasse 85, D-22603 Hamburg, Germany, Institute of Crystallography, Russian Academy of Sciences, Leninsky pr. 59, 117333 Moscow, Russia, and Universität Osnabrück, Fachbereich Biologie/Chemie, Abteilung Mikrobiologie and Abteilung Zoophysiologie, D-49069, Osnabrück, Germany

Received October 2, 1998; Revised Manuscript Received November 9, 1998

ABSTRACT: The V_1 ATPase from the tobacco hornworm *Manduca sexta* and the *Escherichia coli* F_1 ATPase were characterized by small-angle X-ray scattering (SAXS). The radii of gyration (R_g) of the complexes were 6.2 ± 0.1 and 4.7 ± 0.02 nm, respectively. The shape of the *M. sexta* V_1 ATPase was determined ab initio from the scattering data showing six masses, presumed to be the A and B subunits, arranged in an alternating manner about a 3-fold axis. A seventh mass with a length of about 11.0 nm extends perpendicularly to the center of the hexameric unit. This central mass is presumed to be the stalk that connects V_1 with the membrane domain (V_O) in the intact V_1V_O-ATPase. In comparison, the shape of the F_1 ATPase from *E. coli* possesses a quasi-3-fold symmetry over the major part of the enzyme. The overall asymmetry of the structure is given by a stem, assumed to include the central stalk subunits. The features of the V_1 and F_1 ATPase reveal structural homologies and diversities of the key components of the complexes.

Some biomolecular assemblies consist of a mosaic of globular structural units including domain or supersecondary structures. These structural units also serve as functional units that play specific roles in the activity. V- and F-ATPases represent clear examples of mosaic structures. They belong to a class of pumps that couple synthesis or hydrolysis of ATP to the translocation of H^+ or Na^+ across the membrane. Each enzyme consists of a peripheral part, V_1 or F_1, that contains the catalytic sites and a membrane-bound part, V_O or F_O, that conducts the ion flow (*1*−*3*). The two major catalytic subunits in the V_1 ATPase (*A* and *B*) with a stoichiometry of A_3B_3 and in the F_1 ATPase ($\alpha_3\beta_3$) have more than 25% primary sequence similarity, whereas it is difficult to identify V_1 subunits that would have any similarity to the smaller polypeptides of F_1 even though the sequences of most of these subunits have been determined (*4*, *5*).

The smaller V_1 subunits C, D, E, F, and G are described as "stalk" subunits (*6*) and appear to bridge the V_1 and V_O parts as seen in electron microscopy images of V ATPase-containing membranes (*7*, *8*). More structural information is available on the F-ATPases. The recently determined high-resolution structures of the $\alpha_3\beta_3\gamma$ subcomplex of the beef heart mitochondria (*9*) and rat liver mitochondria F_1 part (*10*) provide a picture in which the three α and β subunits are arranged in a hexagon around a part of subunit γ. The latter extends from the bottom of F_1 into a stalk that separates the F_1 and membrane-embedded F_O parts. Unfortunately, in the two crystal forms of F_1, the smaller F_1 subunits δ and ϵ are disordered (*9*, *10*).

Here, we report for the first time structural studies of the V_1 ATPase from the tobacco hornworm *Manduca sexta* in solution using small-angle X-ray scattering (SAXS).[1] The overall structure of the V_1 ATPase allows a comparison with the shape of the *Escherichia coli* F_1 ATPase determined in close to physiological conditions.

EXPERIMENTAL PROCEDURES

Scattering Experiments and Data Analysis. The synchrotron radiation X-ray scattering data were collected on the X33 camera (*11*−*13*) of the European Molecular Biology Laboratory (EMBL) on the storage ring DORIS III of the Deutsches Elektronen Synchrotron (DESY) using multiwire proportional chambers with delay line readout (*14*). At the sample−detector distance of 3.8 m and the wavelength λ = 0.15 nm the range of momentum transfer 0.14 $nm^{-1} < s <$ 2.1 nm^{-1} was covered (s is the modulus of the momentum transfer $\boldsymbol{s}$, $s = 4\pi \sin\theta/\lambda$ where 2θ is the scattering angle). The data were normalized to the intensity of the incident beam and corrected for the detector response, the scattering

* To whom correspondence should be addressed: Dr. Gerhard Grüber, Universität Osnabrück, Fachbereich Biologie/Chemie, D-49069 Osnabrück, Germany. Phone: +49/(0)541 969 2809. Fax: +49/(0)-541 969 2870. E-mail: grueber@biologie.uni-osnabrueck.de.

† This research was supported by the Deutsche Forschungsgemeinschaft (SFB171/B4, Wi698), by Human Frontiers (HFSP, RG0571/1996-M), by National Institutes of Health Grant Al 22444, by International Association for the Promotion of Cooperation with Scientists from the Independent States of the Former Soviet Union (INTAS) Grant No. 96-1115 (to D.I.S. and M.H.J.K.), and the EU Biotechnology Program (Grant BIO4-CT97-2143 to D.I.S.).

‡ EMBL-Outstation Hamburg.

§ Institute of Crystallography, Russian Academy of Sciences.

|| Abteilung Mikrobiologie, Universität Osnabrück.

⊥ Abteilung Zoophysiologie, Universität Osnabrück.

[1] Abbreviations: SAXS, small-angle X-ray scattering; SDS, sodium dodecyl sulfate.

10.1021/bi982367a CCC: $15.00
Published on Web 12/03/1998

of the buffer was subtracted, and the difference curves were scaled for concentration using the program SAPOKO (Svergun & Koch, unpublished results).

The maximum dimensions D_{max} of the V_1 and F_1 ATPase were estimated from the experimental curves using the orthogonal expansion program *ORTOGNOM* (*15*). The distance distribution functions *p(r)* and the radii of gyration R_g were evaluated by the indirect Fourier transform program *GNOM* (*16*, *17*). The Porod volumes V_p were calculated from the processed (backtransformed from the *p(r)*) scattering curves as described by Feigin and Svergun (*18*), Ch. 3.3.3.

The low-resolution particle envelopes were restored from the experimental data using the ab initio shape determination procedure of Svergun and Stuhrmann (*19*) and Svergun et al. (*20*, *21*). The particle shape is represented by an angular envelope function $r = F(\omega)$ where (r,ω) are spherical coordinates. The envelope is parametrized as

$$F(\omega) = \sum_{l=0}^{L} \sum_{m=-l}^{l} f_{lm} Y_{lm}(\omega) \qquad (1)$$

where $Y_{lm}(\omega)$ are spherical harmonics and the multipole coefficients f_{lm} are complex numbers. Series (1) contains in the general case $M = (L + 1)^2$ parameters and provides a spatial resolution of approximately $\delta r = \sqrt{5}\pi R_g/[\sqrt{3}(L + 1)]$. The scattering intensity of the envelope is evaluated as (*22*)

$$I(s) = 2\pi^2 \sum_{l=0}^{\infty} \sum_{m=-l}^{l} |A_{lm}(s)|^2 \qquad (2)$$

where the partial amplitudes $A_{lm}(s)$ are calculated from the coefficients f_{lm} using the recurrence relation of ref *19*. These coefficients can be determined by minimizing the discrepancy between the calculated and the experimental curves

$$R_I^2 = \frac{\sum_{j=1}^{N} \{W(s_j)[I(s_j) - I_{exp}(s_j)]\}^2}{\sum_{j=1}^{N} [W(s_j) I_{exp}(s_j)]^2} \qquad (3)$$

where N is a number of experimental points and the weighting function is $W(s_j) = s_j^2/[\sigma(s_j)/I_{exp}(s_j)]$, where $I_{exp}(s_j)$ and $\sigma(s_j)$ are the experimental intensity and its standard deviation in the j-th point, respectively.

The major parts of the molecules of V_1 and F_1 ATPase are known to possess quasi-3-fold symmetry (*7*, *23*). This symmetry restriction leads to selection rules for the coefficients f_{lm} and was employed to reduce the number of parameters in series 1. Thus, at a resolution of $L = 5$ the description of a symmetric envelope using series 1 requires $M = 12$ parameters instead of $M = 36$ for the general case. The shape determination was performed assuming a 3-fold symmetry by the minimization program *SASHA* (*20*, *21*). The program starts from a spherical initial approximation and fits the experimental data by a nonlinear optimization procedure with additional penalties to keep the particle surface smooth and its envelope function positive definite.

Other Methods. Purification of the V_1 ATPase from *M. sexta*, protein determination with Amido Black, standard SDS−polyacrylamide gel electrophoresis, and ATPase activity measurements were performed as described previously (*24*, *25*). The purification of *E. coli* F_1 ATPase was accomplished according to Grüber et al. (*26*). The protein concentration of F_1 was determined according to Dulley and Grieve (*27*), and ATP hydrolysis was measured as described by Fiske and Subbarow (*28*) and Arnold et al. (*29*).

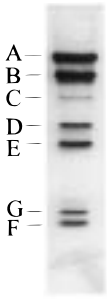

FIGURE 1: V_1 ATPase purified from starving *Manduca sexta* larvae. V_1 ATPase (1 μg) was applied to an SDS−polyacrylamide gel, and the subunits were stained with silver.

RESULTS AND DISCUSSION

For the experiments described here the V_1 ATPase of the larval *M. sexta* midgut was isolated to homogeneity (*24*). Figure 1 presents an SDS-polyacrylamide gel (17.5% total and 0.4% cross-linked acrylamide) of the V_1 ATPase used in the small-angle X-ray studies. The enzyme contains the seven subunits A, B, C, D, E, F, and G. At first glance, subunit C appears to be present in substoichiometric amounts. However, as our data will show, the V_1 complex is homogeneous; moreover, as shown previously, the intensity of subunit C in silver-stained SDS−polyacrylamide gels is weak in comparison to gels stained with Coomassie blue (*30*, *31*). So far there is no unequivocal indication for the presence of subunit H which is a constituent member of the catalytic V_1 complex in yeast (Vma13p (*32*)) and in bovine clathrin-coated vesicles (SFD (*33*)). The ATP hydrolysis rates as isolated were 1.9 μmol of ATP hydrolyzed per milligram of protein per minute in the presence of 25% methanol. Figure 2 shows the experimental solution X-ray scattering profile of 10 mg of V_1 ATPase per mL. The asymmetric profile of the distance distribution function $p(r)$ is characterized by the radius of gyration, $R_g = 6.2 \pm 0.1$ nm, peak position at 6.7 $\pm$ 0.3 nm and the maximum particle dimension, D_{max}, at 22.0 $\pm$ 0.1 nm (see Figure 3). This indicates that, in the present solvent condition, the structure of the V_1 ATPase is rather elongated. Comparison of the normalized forward scattering with the values obtained for a reference solution of bovine serum albumin yields a molecular mass of 550 $\pm$ 20 kDa, in agreement with a molar ratio of A_3:B_3:C:D:E:F:G_3 and apparent molecular masses of 67, 56, 40, 32, 28, 14, and 16 kDa. These indicate that aggregation of the enzyme complex does not occur at the concentrations used. The Porod volume of V_1 is 970 $\pm$ 30 nm^3, and this is in good agreement with the molecular mass estimation. The hydrolytic activity of the V_1 ATPase after exposure to X-rays was 2.2 μmol of ATP hydrolyzed per milligram per minute, indicating that the enzyme was not damaged by X-rays.

The low-resolution envelope of V_1 was determined ab initio from the experimental data as described in Materials and Methods assuming a 3-fold symmetry. The maximum

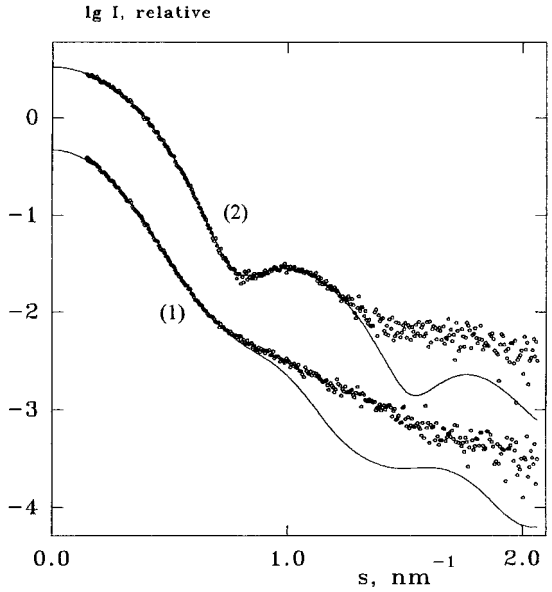

FIGURE 2: Experimental and calculated curves of the V_1 (1) and F_1 ATPase (2): dots, experimental data; solid lines, scattering from the restored envelopes in Figure 3. The V_1 curves are displaced down one logarithmic unit for clarity. The V_1 ATPase (10 mg/mL) was dissolved in 20 mM Tris-MOPS (pH 8.1) and 30 mM NaCl. The X-ray scattering of the *E. coli* F_1 ATPase (10 mg/mL) was measured after incubation (10 min) with 2 mM MgATP (ratio of 1:1) at room temperature.

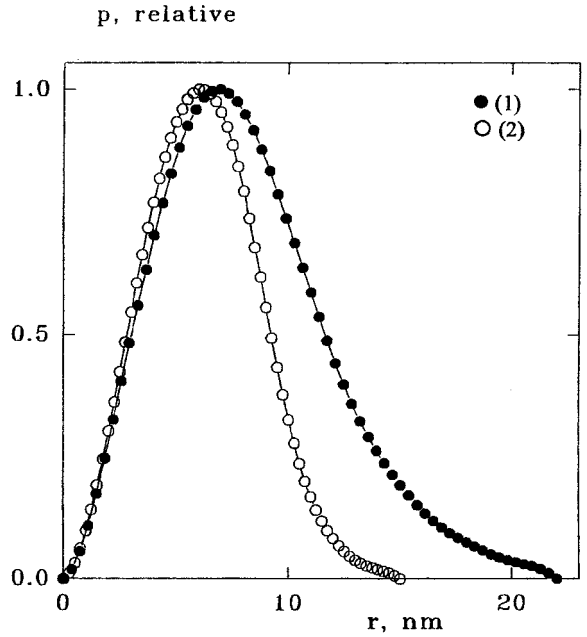

FIGURE 3: Distance distribution functions of V_1 (1) and F_1 ATPase (2) evaluated by the program *GNOM*. The functions are normalized to a maximum value of unity for better visualization.

order of harmonics L in series 1 was chosen to keep the number of free parameters M close to the number of Shannon channels in the experimental data $N_s = s_{max}D_{max}/\pi$. As shown by Svergun et al. (*20*), shape determination is unique when M does not exceed $1.5N_s$. The value of N_s was 14.4 allowing the use of $L = 6$ ($M = 17$) for the restoration. The restored envelope of V_1 (spatial resolution 3.6 nm) is presented in Figure 4. The final agreement to the experimental data is displayed in Figure 2, yielding a R_I value of 2.5×10^{-2}. The R_I values were evaluated using eq 3 in the entire range. Note that, as the scattering curves decrease rapidly with s,

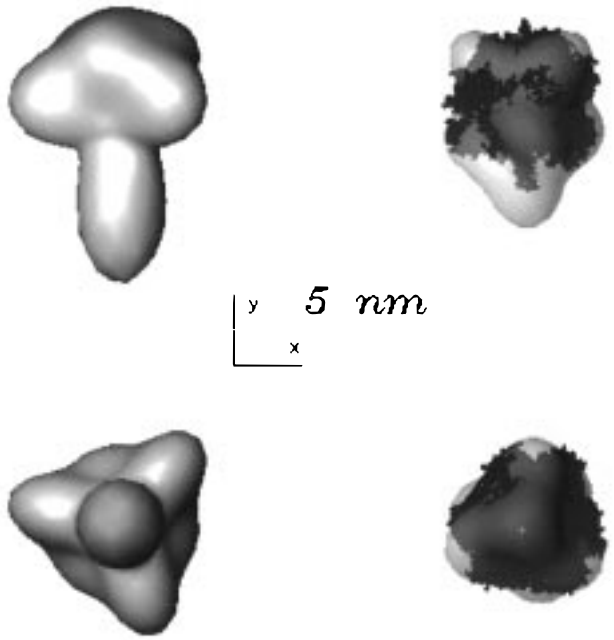

FIGURE 4: Low-resolution envelopes of ATPases: V_1 complex (left panel) and F_1 complex (right panel). The atomic model of the beef heart mitochondria $\alpha_3\beta_3$ subassembly (α_{DP}19−510, α_{TP}25−510, α_E24−510, and β9−474) and the part of subunit γ (γ1−45, γ73−90, and γ209−272 (*9*)) are positioned inside the low-resolution model of the *E. coli* F_1 ATPase (right panel): bottom images, view along the 3-fold axis (Z); top images are rotated counterclockwise around the *X* axis by 90°. The models were displayed on a SUN Workstation using the program *ASSA* (*48*).

the discrepancies in the outer part of the curve contribute less to the entire R factor. The form of the R factor (3) was found to be optimal for low-resolution shape restoration in earlier studies (*34*). The outer part of the scattering curve cannot be fitted neatly, because of the increasing contribution from the scattering due to the internal inhomogeneities at higher angles, and also because of the resolution limitations of the spherical harmonics representation of highly anisometric shapes. However, the deviation at higher angles does not influence the following conclusions about the gross features of the particle shape as those are defined by the initial part of the curve ($s < 1$ nm^{-1}).

The envelope of V_1 ATPase is rather elongated with a globular structure at the top consisting essentially of six masses, assumed to be the subunits A and B, arranged in an alternating manner (see Figure 4). An elongated, symmetrical "stalk" with a length of about 11.0 nm runs perpendicularly to that hexameric mass. These structural features are also those found in images of negatively stained single particles of this V_1 complex showing six major masses of density in a pseudohexagonal arrangement surrounding a central seventh mass (Rademacher, Ruiz, Wieczorek, and Grüber, unpublished data). A stalk of the dimensions shown in Figure 4 could accommodate the mostly α-helical and elongated subunits C, D, E, F, and G (*35*−*39*) with a total molecular mass of about 162 kDa, assuming a stoichiometry of C:D:E:F:G_3. It should be noted that, in comparison to recent electron micrographs of negatively stained V-ATPase from *Clostridium fervidus* (*40*), the headpiece of the *M. sexta* V_1 complex exhibits a more rounded feature. Whether this difference is due to negative staining cannot be decided at present; studies applying cryoelectron microscopic techniques

which help to preserve speciments of the enzyme in their native structure in a thin layer of amourphous ice may solve this problem. Correspondent studies are ongoing in our laboratoury.

Previously, we have characterized the F_1 ATPase (stoichiometry $\alpha_3\beta_3\gamma\delta\epsilon$) from *E. coli* by small-angle X-ray scattering in the presence of 10% glycerol, which prevented the interpretation of the scattering data at larger angles ($s \geq 1.5$ nm^{-1}) (*41*). As demonstrated in the scattering profile in Figure 2 the data could be improved ($0.1 \leq s$ (nm^{-1}) ≥ 2.0) using buffer without glycerol, which allowed the comparison with the scattering profile of the V_1 ATPase described above. The R_g and D_{max} for the F_1 complex have values of 4.7 ± 0.02 and 15.0 ± 0.5 nm, respectively. The Porod volume of F_1 is 640 ± 20 nm^3, in agreement with the molecular mass estimate of 390 ± 20 kDa. The profile of the $p(r)$ function has a peak at 6.1 ± 0.2 nm, and a F_1 molecule thus appears more compact than the V_1 one.

The shape of F_1 ATPase at a resolution of 3.2 nm was evaluated ab initio from its solution scattering curve yielding $R_I = 9.3 \times 10^{-3}$, and a compact envelope function obtained is illustrated in Figure 4. The central part of the envelope has a pronounced 3-fold symmetry and can be identified as the $\alpha_3\beta_3$ subcomplex as described recently ((*41*); see also Figure 4). The overall asymmetry of the structure is given by a short stem at the bottom of the molecule, assumed to include the central stalk subunits γ and ϵ, which are involved in the conformational coupling that links catalytic site events in the $\alpha_3\beta_3$ complex with ion pumping through the F_O sector (*42*−*46*).

The structural parameters and the shape determination of V_1 and F_1 obtained from small-angle X-ray scattering give a well-defined description of the structural features of these complexes. The major differences in the quaternary structure of the two molecules are that the V_1 complex is not only larger but also more anisometric than the F_1 complex. The significant length of the stalk of V_1, which separates the catalytic part from the ion-conducting part, requires conformational coupling of the stalk subunits during ATP hydrolysis. This implies an enzymatic mechanism which postulates movement of stalk subunits or parts of them with respect to one another as well as to the peripheral A and B subunits. The key to understanding the mechanism of catalytic coupling is to characterize the structural changes in the V_1 complex during ATP hydrolysis. If they are sufficiently large, the conformational changes of macromolecular assemblies are better studied in solution to avoid the interference with the packing forces in the crystal on the changes, as already observed in other cases (*47*). Small-angle X-ray scattering combined with other techniques to study these conformational changes in the future should lead to a rational interpretation of the mechanism of conformational coupling.

ACKNOWLEDGMENT

The authors are grateful to Giundula Key, Harald Mikoleit, and Gerlinde Brützel for enzyme preparation.

REFERENCES

1. Stevens, T. H., and Forgac, M. (1997) *Annu. Rev. Cell Dev. Biol. 13*, 779−808.
2. Fillingame, R. H. (1997) *Curr. Opin. Struct. Biol. 6*, 491−498.
3. Dimroth, P. (1997) *Biochim. Biophys. Acta 1318*, 11−51.
4. Nelson, N. (1989) *J. Bioenerg. Biomembr. 21*, 553−571.
5. Bowman, B. J., and Bowman, E. J. (1997) in *The Mycota III. Biochemistry And Molecular Biology* (Brambl and Marzluf, Eds.) pp 57−83.
6. Tomashek, J. J., Graham, L. A., Hutchins, M. U., Stevens, T. H., and Klionsky, D. J. (1997) *J. Biol. Chem. 272*, 26787−26793.
7. Dschida, W. J., and Bowman, B. J. (1992) *J. Biol. Chem. 267*, 18783−18789.
8. Harvey, W. R. (1992) *J. Exp. Biol. 172*, 1−17.
9. Abrahams, J. P., Leslie, A. G. W., Lutter, R., and Walker, J. E. (1994) *Nature 370*, 621−628.
10. Bianchet, M. A., Hullihen, J., Pedersen, P. L., and Amzel, M. L. (1998) *Proc. Natl. Acad. Sci. U.S.A. 95*, 11065−11070.
11. Koch, M. H. J., and Bordas, J. (1983) *Nucl. Instrum. Methods 208*, 461−469.
12. Boulin, C., Kempf, R., Koch, M. H. J., and McLaughlin, S. M. (1986) *Nucl. Instrum. Methods A249*, 399−407.
13. Boulin, C. J., Kempf, R., Gabriel, A., and Koch, M. H. J. (1988) *Nucl. Instrum. Methods A269*, 312−320.
14. Gabriel, A., and Dauvergne, F. (1982) *Nucl. Instrum. Methods 201*, 223−224.
15. Svergun, D. I. (1993) *J. Appl. Crystallogr. 26*, 258−267.
16. Svergun, D. I., Semenyuk, A. V., and Feigin, L. A. (1988) *Acta Crystallogr., Sect. A 44*, 244−250.
17. Svergun, D. I. (1992) *J. Appl. Crystallogr. 25*, 495−503.
18. Feigin, L. A., and Svergun, D. I. (1987) Plenum Press, New York.
19. Svergun, D. I., and Stuhrmann, H. B. (1991) *Acta Crystallogr., Sect. A 47*, 736−744.
20. Svergun, D. I., Volkov, V. V., Kozin, M. B., and Stuhrmann, H. B. (1996) *Acta Crystallogr., Sect. A 52*, 419−426.
21. Svergun, D. I., Volkov, V. V., Kozin, M. B., Stuhrmann, H. B., Barberato, C., and Koch, M. H. J. (1997) *J. Appl. Crystallogr. 30*, 798−802.
22. Stuhrmann, H. B. (1970) *Z. Phys. Chem. 72*, 177−198.
23. Shirakihara, Y., Leslie, A. G. W., Abrahams, J. P., Walker, J. E., Ueda, T., Sekimoto, Y., Kambara, M., Saika, K., Kagawa, Y., and Yoshida, M. (1997) *Structure 5*, 825−836.
24. Gräf, R., Harvey, W. R., and Wieczorek, H. (1996) *J. Biol. Chem. 271*, 20908−20913.
25. Wieczorek, H., Cioffi, M., Klein, U., Harvey, W. R., Schweikl, H., and Wolfersberger, M. G. (1990) *Methods. Enzymol. 192*, 608−616.
26. Grüber, G., Hausrath, A., Sagermann, M., and Capaldi, R. A. (1997) *FEBS Lett. 410*, 165−168.
27. Dulley, J. R., and Gieve, P. (1975) *Anal. Biochem. 64*, 136−147.
28. Fiske, C. H., and Subarow, Y. (1925) *J. Biol. Chem. 271*, 32623−32628.
29. Arnold, A., Wolf, H. U., Ackermann, B. P., and Bader, H. (1976) *Anal. Biochem. 71*, 209−213.
30. Sumner, J. P., Dow, J. A. T., Earley, F. G. P., Klein, U., Jäger, D., and Wieczorek, H. (1995) *J. Biol. Chem. 270*, 5649−5653.
31. Merzendorfer, H., Gräf, R., Huss, M., Harvey, W. R., and Wieczorek, H. (1997) *FEBS Lett. 411*, 239−244.
32. Ho, M. N., Hirata, R., Umemoto, N., Ohya, Y., Takatsuki, A., Stevens, T. H., and Anraku, Y. (1993) *J. Biol. Chem. 268*, 18286−18292.
33. Xie, X. S., Crider, B. P., Ma, Y. M., and Stone, D. K. (1994) *J. Biol. Chem. 269*, 25809−25815.
34. Svergun, D. I., Volkov, V. V., Kozin, M. B., Stuhrmann, H. B., Barberato, C., and Koch, M. H. J. (1997) *J. Appl. Crystallogr. 30*, 798−802.
35. Nelson, H., Mandiyan, S., and Nelson, N. (1995) *Proc. Natl. Acad. Sci. U.S.A. 92* (2), 497−501.
36. Bowman, E. J., Steinhardt, A., and Bowman, B. J. (1995) *Biochim. Biophys. Acta 1237*, 95−98.
37. Hunt, I. E., and Bowman, B. J. (1997) *J. Bioenerg. Biomembr. 29*, 533−540.
38. Lepier, A., Gräf, R., Azuma, M., Merzendorfer, H., Harvey, W. R., and Wieczorek, H. (1996) *J. Biol. Chem. 271*, 8502−8508.

39. Gräf, R., Lepier, A., Harvey, W. R., and Wieczorek, H. (1994) *J. Biol. Chem. 269*, 3767−3774.
40. Boekema, E. J., Ubbink-Kok, T., Lolkema, J. S., Brisson, A., and Konings, W. N. (1997) *Proc. Natl. Acad. Sci. U.S.A. 94*, 14291−14293.
41. Svergun, D. I., Aldag, I., Sieck, T., Altendorf, K., Koch, M. H. J., Kane, D. J., Kozin, M. B., and Grüber, G. (1998) *Biophys. J. 75*, 2212−2219.
42. Cross, R. L., and Duncan, T. M. (1996) *J. Bioenerg. Biomembr. 28*, 403−408.
43. Junge, W., Lill, H., and Engelbrecht, S. (1997) *Trends Biochem. Sci. 22*, 420−423.
44. Fillingame, R. H. (1997) *J. Exp. Biol. 200*, 217−224, 1997.
45. Kinosita, K., Jr., Yasuda, R., Noji, H., Ishiwata, S., and Yoshida, M. (1998) *Cell 93*, 21−24.
46. Capaldi, R. A., Aggeler, R., Wilkens, S., and Grüber, G. (1996) *J. Bioenerg. Biomembr. 28*, 397−401.
47. Svergun, D. I., Barberato, C., Koch, M. H. J., Fetler, L., and Vachette, P. (1997) *Proteins 27*, 110−117.
48. Kozin, M. B., Volkov, V. V., and Svergun, D. I. (1997) *J. Appl. Crystallogr. 30*, 811−815.

BI982367A